



Van Yüzüncü Yıl Üniversitesi  
Mühendislik Fakültesi Dergisi  
<https://dergipark.org.tr/tr/pub/vyuyumfd>



## Metaheuristic Algorithms Based PID Controller Tuning Approach for Inverted Pendulum System

Ahmet Sadık DURU<sup>a,\*</sup>

<sup>a</sup> Department of Mechanical Engineering, Faculty of Engineering and Natural Sciences, Ankara Yıldırım Beyazıt University, Ankara, Turkey, ORCID: 0000-0001-9142-9344

### ABSTRACT

Proportional, integral, derivative (PID) controllers, also known as proportional integral derivative controllers, are frequently used to regulate system outputs. PID parameter settings have a significant impact on system performance. Various methods are used to determine the parameters, which have disadvantages. Metaheuristic optimization algorithms have been used to overcome these disadvantages. This study obtained a linearized mathematical model of the inverted pendulum system. Controller parameters were obtained by applying the Ziegler-Nichols method to the linear model of the system. Then, the PID gain parameters of the inverted pendulum system were tuned by three different metaheuristic optimization methods, which are particle swarm optimization (PSO), sine cosine optimization (SCA), and gray wolf optimization (GWO). It has been observed that the performance of the PID controller has increased significantly because of adjusting the control parameters with metaheuristic optimization algorithms. This study compared the results obtained from the integrated absolute error (IAE) fitness function due to the application of PSO, SCA, and GWO methods. Convergence graphs of PSO, SCA, and GWO algorithms were obtained, and the convergence speed of the GWO algorithm was faster than the other two methods applied.

**Keywords:** Inverted pendulum, PID parameters tuning, Metaheuristic, Particle swarm optimization, Sine cosine optimization algorithm, Gray wolf optimization algorithm.

## Ters Sarkaç Sistemi için Meta Sezgisel Algoritmalarla Dayalı PID Denetleyici Ayarlama Yaklaşımı

Ahmet Sadık DURU<sup>a,\*</sup>

<sup>a</sup>Makine Mühendisliği Bölümü, Mühendislik ve Doğa Bilimleri Fakültesi, Ankara Yıldırım Beyazıt Üniversitesi, Ankara, Türkiye, ORCID: 0000-0001-9142-9344

### ÖZET

Oransal integral türev kontrolörleri olarak da bilinen PID kontrolörleri, sistem çıkışlarını düzenlemek için sıklıkla kullanılır. PID parametre ayarlarının sistem performansı üzerinde önemli bir etkisi vardır. Bu parametrelerin belirlenmesinde kullanılan çeşitli yöntemler mevcut olup bu yöntemlerin dezavantajları bulunmaktadır. Bu olumsuzlukların üstesinden gelmek için meta sezgisel optimizasyon algoritmaları kullanılmıştır. Bu çalışmada ters sarkaç sisteminin doğrusallaştırılmış matematik modeli elde edilmiştir. Sistemin doğrusal modeline Ziegler-Nichols metodu uygulanarak kontrolcü parametreleri elde edilmiştir. Daha sonra ters sarkaç sisteminin PID kazanç parametreleri, parçacık sürüsü optimizasyonu (PSO), sinüs kosinüs optimizasyonu (SCA) ve gri kurt optimizasyonu (GWO) olmak üzere üç farklı meta sezgisel optimizasyon yöntemiyle ayarlanmıştır. Meta sezgisel optimizasyon algoritmalarıyla kontrol parametrelerinin ayarlanması sonucu PID kontrolcünün performansında önemli ölçüde artış meydana geldiği görülmüştür. Bu çalışmada PSO, SCA ve GWO yöntemlerinin uygulanması sonucu mutlak hata integrali uygunluk fonksiyonundan elde edilen sonuçlar karşılaştırılmıştır. PSO, SCA ve GWO metotlarının yakınsama grafikleri elde edilmiş olup GWO algoritmasının yakınsama hızı uygulanan diğer iki yönteme göre daha hızlı sonuç vermiştir.

**Anahtar Kelimeler:** Ters sarkaç, PID parametrelerinin ayarlanması, Meta sezgisel optimizasyon, Parçacık sürü optimizasyonu, Sinüs kosinüs optimizasyon algoritması, Gri kurt optimizasyon algoritması.

## 1. Introduction

Numerous controller methods have been developed in the field of control theory. Nevertheless, despite the plethora of options available, the PID controller continues to be extensively implemented in the industry. Broad application use is primarily due to its ease of implementation and successful control performance. A mathematical model must be developed based on the system's physical structure to create an effective controller. The mathematical models of many engineering systems have a non-linear complex structure [1]; the system must be linear to implement the PID controller. PID controller performance varies depending on gain parameters. Various methods have been used to adjust PID gain parameters. These methods can be listed as follows: the Ziegler-Nichols method [2], which provides an empirical solution; the root-locus design [3], another analytical way; and finally, optimization methods were used. The gain parameters adjusted by the Ziegler-Nichols method are not optimum values even if the controller gives good results. Manually adjusting control parameters is not an effective method today. There are many disadvantages in determining parameters using the root locus. The root-locus method gives better results in linear time-invariant systems, and the root locus is more effective in single-input, single-output (SISO) systems. Still, its applicability could be better in multi-input multi-output (MIMO) systems. Uncertainties in the mathematical model affect the accuracy of the analysis. In addition, while the root-locus system provides information about the positions of the roots and zeros in the complex plane, it does not give information on disturbance inputs, noise, or steady-state errors that affect control performance.

As the physical structure of systems becomes complex, finding solutions becomes difficult. Many methods have been developed to overcome these difficulties. Metaheuristic methods can provide practical solutions in systems where the number of parameters to be optimized is large. Since metaheuristic methods search for answers with multiple agents, they do not confuse local optimum points with global solutions. In other words, they give good results even when the objective function could be flatter and smoother. There are many studies in the literature in which PID parameters are optimized using metaheuristic methods. If some of these studies are reviewed, genetic algorithm (GA) [4,5,6], artificial bee colony algorithm (ABC) [7], ant colony optimization algorithm (ACO) [8], particle swarm optimization (for adjusting PID parameters) PSO [9], whale optimization algorithm (WOA) [10], ant lion optimizer (ALO) [11] and sine cosine optimization algorithm (SCA) [12] methods were used.

In the literature, many metaheuristic optimization methods have been used to increase the controller performance of the inverted pendulum. A study performed non-linear control using the inverted pendulum particle swarm optimization-based model predictive control method with planar motion [13]. In another study, an inverted pendulum was applied to the fuzzy logic controller with a modified genetic algorithm [14]. In another study, the parameters of two different PID controllers of an inverted pendulum were determined by the PSO method, and experimental studies were carried out [15]. In another study where the LQR controller controlled the inverted pendulum system, the ABC algorithm was applied to improve the controller performance. LQR controller parameters were determined with the ABC algorithm [16]. In a study where the integral sliding mode controller was used to control the inverted pendulum system, the performance of integral sliding mode control (ISMC) was improved with WOA. WOA-ISMC showed better controller performance than the first comparisons [17].

This study used three metaheuristic optimization methods to determine the control parameters of the inverted pendulum performing planar motion. The controller performance has increased thanks to the applied PSO-PID, SCA-PID, and GWO-PID methods. The performance increase was confirmed by IAE and ISE methods, which are statistical error analyses. In addition, comparisons were made between PSO, SCA, and GWO methods according to their performance and convergence speed. Since the relevant techniques can be applied to different controllers, metaheuristic methods can be used in the control process of other systems.

## 2. Material and Method

### 2.1 Mathematical Model

The system to be controlled consists of an inverted pendulum mounted on a cart. The inverted pendulum system is widely used in the literature to test the performance of a control algorithm. If the pendulum is not controlled, it cannot remain balanced in a vertical position. Control input is generated through a cart to balance the pendulum vertically. In this study, an inverted pendulum is balanced with a cart moving in two dimensions horizontally.

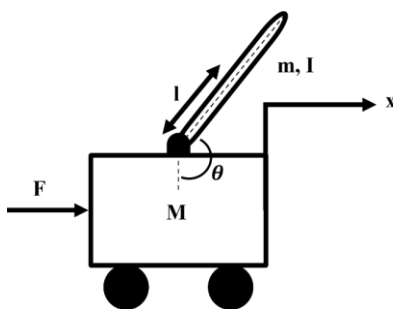


Figure 1. Inverted pendulum system.

In the inverted pendulum system in Figure 1, the control input is the force  $F$ , and the outputs are  $\theta$  for the pendulum and  $x$  for the cart; that is, this system is a single-input multi-output (SIMO).

Table 1. Parameters of the inverted pendulum system

| Symbol   | Explanation                                 | Value                  |
|----------|---|------------------------|
| $M$      | Cart's mass                                 | 0.5 kg                 |
| $m$      | The pendulum's mass                         | 0.2 kg                 |
| $b$      | Cart friction coefficient                   | 0.1 N/m/sec            |
| $l$      | Distance from the pendulum's center of mass | 0.3 m                  |
| $I$      | The pendulum's mass moment of inertia       | 0.006 kgm <sup>2</sup> |
| $F$      | Force exerted on the cart                   | -                      |
| $x$      | Coordinates for cart position               |                        |
| $\theta$ | The angle of the pendulum from the vertical |                        |

The non-linear dynamic equations forming the inverted pendulum system were obtained using the Newton method. The system's free body diagram was obtained using the Newton method to perform dynamic analysis, as shown in Figure 2. The pendulum's weight and the cart's movement create a horizontal  $N$  force and a vertical  $P$  force.

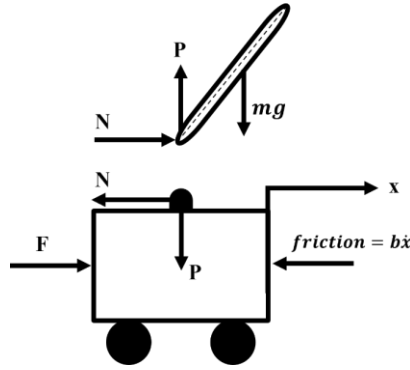


Figure 2. Free body diagram of inverted pendulum system.

Equation 1 is obtained due to the sum of the forces on the cart in the horizontal direction from Figure 2.

$$M\ddot{x} + b\dot{x} + N = F \quad (1)$$

Equation 2 is obtained by summing the horizontal forces on the pendulum from the free-body diagram.

$$N = m\ddot{x} + ml\ddot{\theta} \cos \cos \theta - ml\dot{\theta}^2 \sin \sin \theta \quad (2)$$

When equation 2 is substituted in equation 1, equation 3 is obtained as follows.

$$(M + m)\ddot{x} + b\dot{x} + ml\ddot{\theta} \cos \cos \theta - ml\dot{\theta}^2 \sin \sin \theta = F \quad (3)$$

$$P \sin \sin \theta + N \cos \cos \theta - mg \sin \sin \theta = ml\ddot{\theta} + m\ddot{x} \cos \cos \theta \quad (4)$$

The sum of the moments concerning the pendulum's center of gravity can be written as in equation 5 to eliminate the P and N terms in equation 4. If the expressions in Equation 4 and 5 are combined, equation 6 is obtained.

$$-Pl \sin \sin \theta - Nl \cos \cos \theta = I\ddot{\theta} \quad (5)$$

$$(I + ml^2)\ddot{\theta} + mgl \sin \sin \theta = -ml\ddot{x} \cos \cos \theta \quad (6)$$

In particular, the equations are linearized around the vertically upward equilibrium position  $\theta=\pi$ . The system is assumed to remain within a narrow region of this equilibrium. Under control, it is ideal that the pendulum deviates no more than 15 degrees from the vertical position; therefore, this assumption should be valid. Assume that  $\varphi$  represents the pendulum's positional divergence from equilibrium and that  $\theta=\pi+\varphi$ . Assuming a slight deviation ( $\varphi$ ) from equilibrium, the nonlinear functions in system equations can be approximated using small angles:

$$\cos \cos \theta = \cos \cos (\pi + \varphi) \approx -1 \quad (7)$$

$$\sin \sin \theta = \sin \sin (\pi + \varphi) \approx -\varphi \quad (8)$$

$$\dot{\theta}^2 = \dot{\varphi}^2 \approx 0 \quad (9)$$

When the equations 7, 8, and 9 given above are written in their place, equations 3 and 6 turn into the linear form as in equations 10 and 11.

$$(I + ml^2)\ddot{\varphi} - mgl\varphi = ml\ddot{x} \quad (10)$$

$$(M + m)\ddot{x} + b\dot{x} - ml\ddot{\varphi} = F \quad (11)$$

## 2.2 Transfer Function and State Space Model

The Laplace transform is applied to equations 10 and 11, assuming zero initial conditions to obtain the transfer function to control the inverted pendulum system.

$$(I + ml^2)\varphi(s)s^2 - mgl\varphi(s) = mlX(s)s^2 \quad (12)$$

$$(M + m)X(s)s^2 + bX(s)s - ml\varphi(s)s^2 = F(s) \quad (13)$$

After the necessary operations are done, the pendulum and cart transfer functions are obtained as in equations 14 and 15. Since the system consists of two elements and has a single input and multiple outputs, the number of transfer functions is two.

$$T_{Pendulum}(s) = \frac{\varphi(s)}{F(s)} = \frac{\frac{ml}{q}s}{s^3 + \frac{b(I+ml^2)}{q}s^2 - \frac{(M+m)mgl}{q}s - \frac{bmgI}{q}} \quad \left[ \frac{rad}{N} \right] \quad (14)$$

$$T_{Cart}(s) = \frac{X(s)}{F(s)} = \frac{\frac{(I+ml^2)s^2 - gml}{q}}{s^4 + \frac{b(I+ml^2)}{q}s^3 - \frac{(M+m)mgl}{q}s^2 - \frac{bmgI}{q}} \quad \left[ \frac{m}{N} \right] \quad (15)$$

The following matrices are obtained when linearized equations of motion are arranged in the state space form and written instead of the values in Table 1.

$$\begin{bmatrix} \dot{x} \\ \ddot{x} \\ \dot{\varphi} \\ \ddot{\varphi} \end{bmatrix} = \begin{bmatrix} 0 & 1 & 0 & 0 \\ 0 & -0.1818 & 2.673 & 0 \\ 0 & 0 & 0 & 1 \\ 0 & -0.4545 & 31.18 & 0 \end{bmatrix} \begin{bmatrix} x \\ \dot{x} \\ \varphi \\ \dot{\varphi} \end{bmatrix} + \begin{bmatrix} 0 \\ 1.818 \\ 0 \\ 4.545 \end{bmatrix} u \quad (16)$$

$$y = \begin{bmatrix} 1 & 0 & 0 & 0 \\ 0 & 0 & 1 & 0 \end{bmatrix} \begin{bmatrix} x \\ \dot{x} \\ \varphi \\ \dot{\varphi} \end{bmatrix} + \begin{bmatrix} 0 \\ 0 \end{bmatrix} u \quad (17)$$

Since the inverted pendulum system has two control outputs ( $x$  and  $\varphi$ ), it is more convenient to use the state-space representation.

## 2.3 PID Controller Design

PID controller is a feedback controller widely used in industrial automation and engineering. A PID controller is frequently preferred because it is easier to implement than other control methods. In this study, two PID controllers were designed to control the pendulum's angle and the cart's position. The time domain expression of the designed controller equations is given below, and the block diagram is designed as in Figure 3.

$$u_p = K_{p_p} e_\theta(t) + K_{d_p} \frac{de_\theta(t)}{dt} + K_{i_p} \int e_\theta(t) dt \quad (18)$$

$$u_c = K_{p_c} e_c(t) + K_{d_c} \frac{de_c(t)}{dt} + K_{i_c} \int e_c(t) dt \quad (19)$$

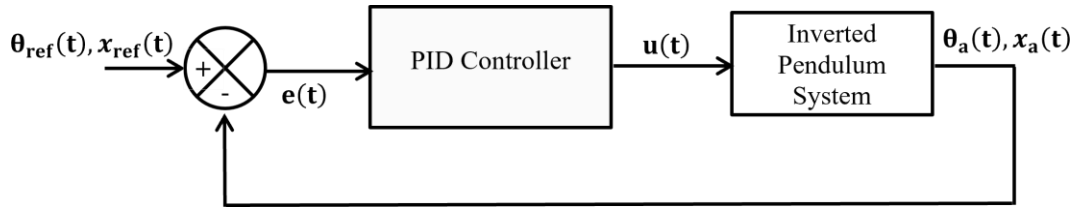


Figure 3. Conventional PID control block diagram for inverted pendulum.

Here,  $e_\theta(t)$  and  $e_c(t)$  indicate the pendulum angle error and cart position error, respectively. PID gain parameters  $K_{pp}$ ,  $K_{dp}$ ,  $K_{ip}$ ,  $K_{pc}$ ,  $K_{dc}$ , and  $K_{ic}$  were determined according to the Ziegler Nichols method.

## 2.4 Tuning PID Parameters Using Metaheuristic Algorithms

There is a coupled relationship between the dynamic equations of the pendulum and cart that make up the inverted pendulum system. Therefore, PID gain parameters directly affect the stability of the entire system. For a high-performance controller design, it is crucial to determine PID gain parameters correctly. Determining these gain coefficients is a mathematically challenging task and does not consistently achieve success. In this study, the gain coefficients of the controller were determined by metaheuristic optimization algorithms to increase the controller's performance. This study determined PID gain parameters using PSO, SCA, and GWO algorithms, respectively.

## 2.5 Fitness Function

The objective function used aims to minimize errors due to controlling the system. The fitness function of the optimized PID controller was determined as an integrated absolute error (IAE). The same fitness function was used for each metaheuristic optimization algorithm used in the study. Fitness function equations are given below.

$$IAE = \int_0^{\infty} |e(t)| dt \quad (20)$$

$$IAE_{pendulum} = \sum_t |\theta_{ref}(t) - \theta_a(t)| \quad (21)$$

$$IAE_{cart} = \sum_t |x_{ref}(t) - x_a(t)| \quad (22)$$

$$constraint_{1i} \leq gain\_coefficient_i \leq constraint_{2i} \quad (23)$$

Where  $\theta_{ref}(t)$  is reference pendulum angle,  $\theta_a(t)$  is actual pendulum angle,  $x_{ref}(t)$  is reference cart position,  $x_a(t)$  is actual cart position and  $e(t)$  is the difference between the reference value and the actual value. The maximum and minimum value range that PID gain parameters can take is defined by Equation 23.

## 2.6 Particle Swarm Optimization

The PSO method, among the swarm intelligence techniques, resembled the behavior of swarms living in groups and was developed by Kennedy and Eberhart in 1995 [18]. Each individual in the herd is represented as a particle, and these particles constitute possible solutions. The particles all represent the swarm, and each particle is produced randomly. Particles move towards the best solution as they

determine their new location. Therefore, in each iteration, the particles update their position towards the best position ( $p_{best}$ ) they have achieved or according to the particle with the best position in the swarm ( $g_{best}$ ). The fitness function is evaluated according to new positions, and the fitness values of the particles are obtained. The new  $p_{best}$  and  $g_{best}$  values are determined by considering the newly calculated velocities (Equation 24) and positions (Equation 25). The process is terminated if the satisfied termination is met; otherwise, the loop continues, as in Figure 4.

$$v_i(k + 1) = wv_i(k) + c_1r_1(x_i^{p_{best}}(k) - x_i(k)) + c_2r_2(x_i^{g_{best}}(k) - x_i(k)) \quad (24)$$

$$x_i(k + 1) = x_i(k) + v_i(k + 1) \quad (25)$$

Where  $i=1,2, 3, \dots, n$ ,  $w$  is weight and  $r_1, r_2$  are random variables in the range of  $(0,1)$ ,  $c_1$ , and  $c_2$  are the acceleration constants. Their role is to make each particle acceleration move the position of  $p_{best}$  and  $g_{best}$ .

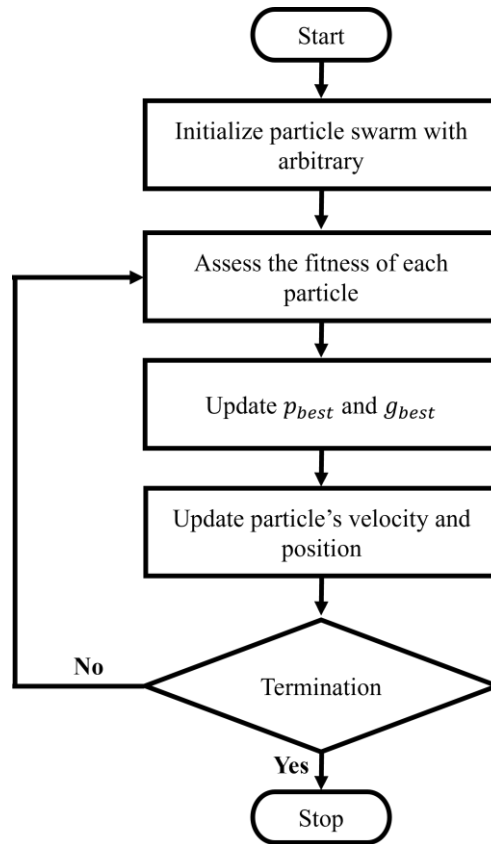


Figure 4. Particle swarm optimization flowchart.

The block diagram showing the design of the PID controller based on PSO is given in Figure 5.

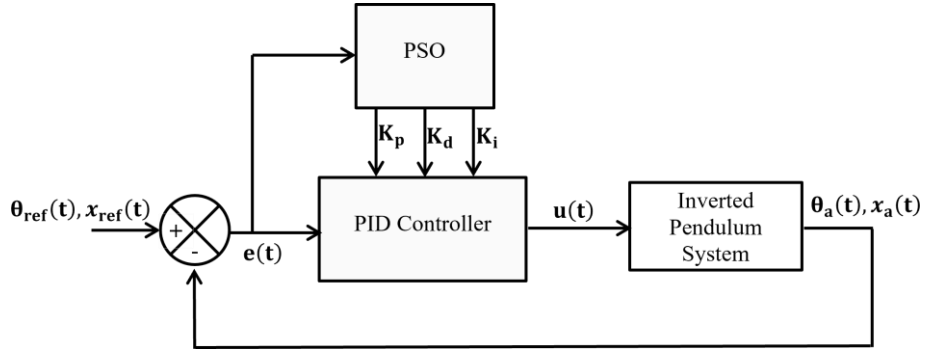


Figure 5. Optimized PID controller block diagram.

## 2.7 Sine Cosine Optimization Algorithm

It was developed by Mirjalili [19], and a set of random solutions is used as the starting point for population-based optimization strategies. This random set is enhanced by a set of rules that form the basis of an optimization technique, which evaluates it periodically according to a fitness function. There is no certainty that a solution will be found in a single run because population-based optimization approaches stochastically search for the optimization issue optimum. However, the possibility of obtaining the global optimum grows with enough random solutions and optimization steps. Regardless of the differences between population-based stochastic algorithms, the optimization process consists of two standard stages: exploration and exploitation. The optimization method swiftly combines random solutions in the solution set with a high randomness rate to identify exciting regions of the search space. However, in the exploitation phase, changes are made gradually to random solutions, and the randomness is much less than in the exploration phase. In this study, position update equations are as in Equation 26 and Equation 27.

$$X_i^{t+1} = X_i^t + r_1 \sin(r_2) |r_3 P_i^t - X_i^t| \quad (26)$$

$$X_i^{t+1} = X_i^t + r_1 \cos(r_2) |r_3 P_i^t - X_i^t| \quad (27)$$

These two equations are used together as in Equation 28.

$$X_i^{t+1} = \begin{cases} X_i^t + r_1 \sin(r_2) |r_3 P_i^t - X_i^t|, & r_4 < 0.5 \\ X_i^t + r_1 \cos(r_2) |r_3 P_i^t - X_i^t|, & r_4 \geq 0.5 \end{cases} \quad (28)$$

where  $X_i^t$  indicates the position of the current solution is in the  $i$ -th dimension at the  $t$ -th iteration,  $r_1$ ,  $r_2$ , and  $r_3$  are random numbers,  $r_4$  is a random number in the range  $[0,1]$ ,  $P_i^t$  is the location of the goal point in the  $i$ -th dimension.

The following position region (or direction of travel) is determined by the parameter  $r_1$ , which may be either outside or inside the area between the solution and the destination. The distance to travel inward or outward from the target is determined by the parameter  $r_2$ . The parameter  $r_3$  assigns a random weight to the destination to stochastically highlight ( $r_3 > 1$ ) or deemphasize ( $r_3 < 1$ ). In the Equation 28,  $r_4$  provides the transition between the sine and cosine components of the equation.

Figure 6 illustrates the effects of the sine and cosine functions in Equations (26) and (27) on the following location. As can be seen in Figure 6, the suggested equations describe the area in the search space between two solutions.



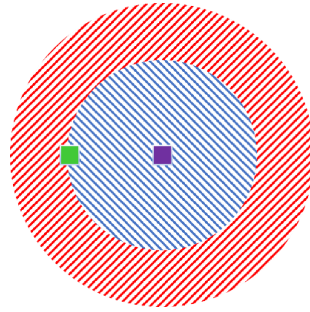


Figure 6. Effects of the sine and cosine functions in Equations (26) and (27) on the following location. The green square shows X (solution), and the purple square shows P (destination). When  $r_1 < 1$ , the next position is in the blue shaded area; otherwise,  $r_1 > 1$  next position is in the red shaded area [19].

The fundamental goal of the sine cosine optimization (SCA) algorithm is to imitate the oscillating behavior of sine and cosine functions to direct the search for the optimum solution. SCA is a very straightforward and understandable optimization procedure that does not need a thorough comprehension of intricate mathematical ideas. It has been used to solve various optimization issues, including function optimization, parameter adjustments, and engineering design. As can be seen in Figure 7, the SCA flowchart was given.

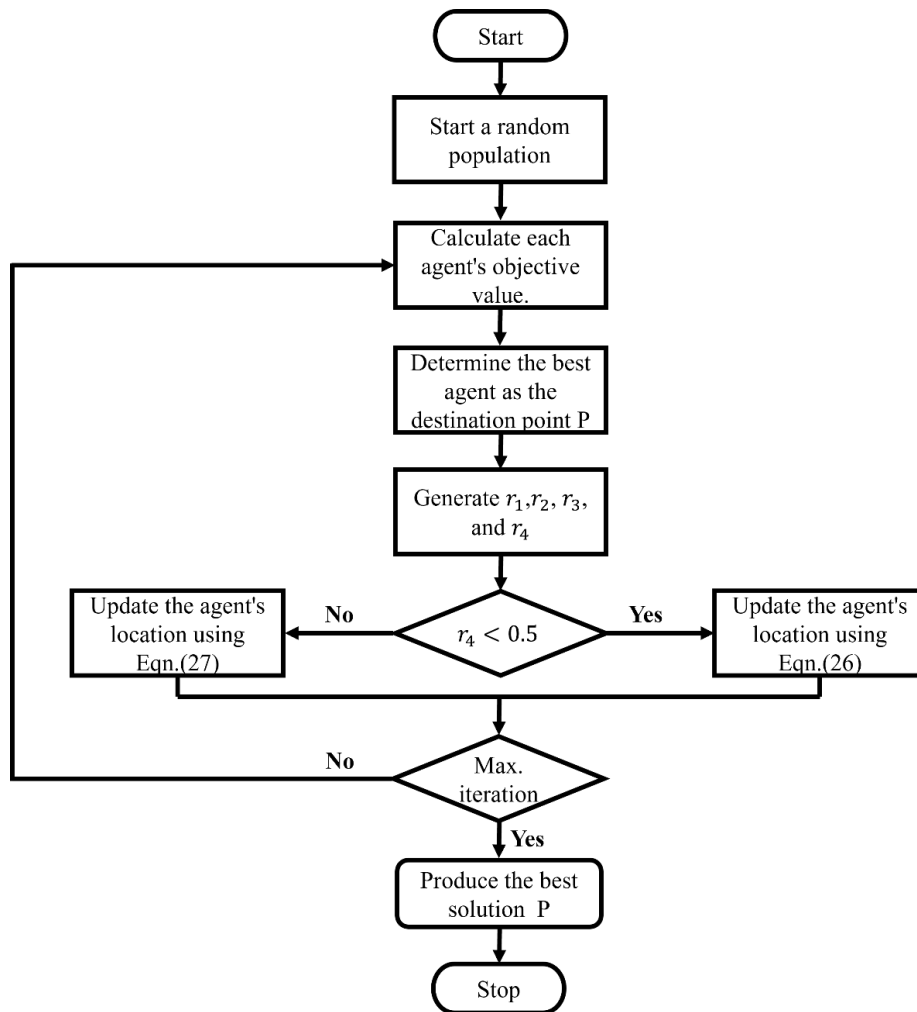


Figure 7. Sine cosine optimization algorithm flow chart.

## 2.8 Gray Wolf Optimization Algorithm

It was developed by Mirjalili et al. [20], considering the hunting mechanism of gray wolves living in groups in nature. The hierarchy among wolves consists of four different categories. As can be seen in Figure 8, this categorical classification is made as alpha, beta, delta, and omega.

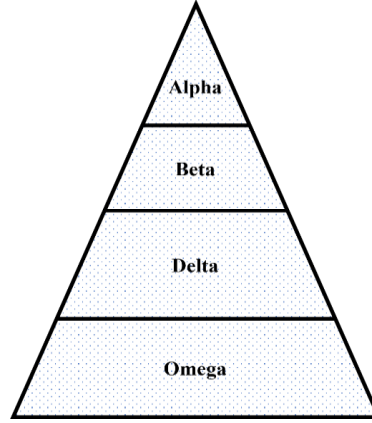


Figure 8. The hierarchy among wolves.

The alpha wolf is the pack's leader and manages the other wolves in the group, determining activities such as sleeping places, waking time, and hunting. At the second level of the hierarchy in the group, the beta wolf serves as the alpha wolf's assistant. The beta wolf organizes the delta and omega wolves with instructions from the alpha wolf. The beta wolf is the strongest candidate to replace the alpha wolf after it gets too old or dies. The hunting behavior model of the wolf pack was used in the design of the optimization algorithm. First, the three best wolves in the group need to be determined. Here, the three best solution sets among the initial solutions are determined. These solutions consist of alpha, beta, and delta solutions. The remaining solutions represent omega solutions. The solution process is continued by alpha, beta, and delta wolves.

Hunting proceeds in a particular order; initially, the prey is followed and surrounded by wolves. The surrounding prey is attacked by alpha, beta, and delta wolves. The positions of alpha, beta, and delta wolves relative to the prey are determined through the Equation (29,30,31) for hunting to take place healthily.

$$\vec{D}_\alpha = |\vec{C}_1 X_{i,\alpha} - X_{i,j}| \quad (29)$$

$$\vec{D}_\beta = |\vec{C}_2 X_{i,\beta} - X_{i,j}| \quad (30)$$

$$\vec{D}_\delta = |\vec{C}_3 X_{i,\delta} - X_{i,j}| \quad (31)$$

$$X_{i,\alpha_{new}} = X_{i,\alpha} - \vec{A}_1 \vec{D}_\alpha \quad (32)$$

$$X_{i,\beta_{new}} = X_{i,\beta} - \vec{A}_2 \vec{D}_\beta \quad (33)$$

$$X_{i,\delta_{new}} = X_{i,\delta} - \vec{A}_3 \vec{D}_\delta \quad (34)$$

$$X_{i,new} = \frac{X_{i,\alpha_{new}} + X_{i,\beta_{new}} + X_{i,\delta_{new}}}{3} \quad (35)$$

Here  $\vec{D}$  is the distance between the prey and the wolf,  $\vec{A} = 2\vec{a}rand - \vec{a}$  vector that determines the wolf's attack on prey,  $\vec{a} = 2 - 2 \frac{t}{stopping\ criterion}$  where  $\vec{a}$  is the vector affecting the distance between the prey and the wolf, coefficient vector  $\vec{C} = 2rand$ ,  $X_{i,j}$  the initial matrix value of the j-th candidate solution of the i-th design variable and  $X_{i,new}$  indicates the new value of the i-th design variable. The condition for

the wolf to attack its prey is fulfilled according to Equation (36). Depending on the vector values  $\vec{A}$ , in cases where the prey is not attacked, the wolf searches for new prey.

$$X_{i,new} = \{|\vec{A}| < 1, \quad X_{i,p} \quad (36)$$

### 3. Results and Discussion

For the control of the inverted pendulum system, a classical PID controller was first designed and the PID gain parameters were determined according to the Ziegler-Nichols method as  $K_{pp} = 100$ ,  $K_{dp} = 20$ ,  $K_{ip} = 1$ ,  $K_{pc} = 20$ ,  $K_{dc} = 10$ , and  $K_{ic} = 2$ . While the pendulum's settling time reached the reference angle at 9.4669 seconds (Figure 10), the cart's settling time reached its reference position at 15.9795 seconds (Figure 9). While the peak value of the pendulum was equal to 0.1960 radians, the peak point of the cart was determined as -0.3011 m. As a result of statistical error analysis on the system, the integrated absolute error (IAE) value was equal to 1.017, while the integrated squared error (ISE) value was obtained as 0.2080.

Secondly, PID gain parameters were obtained by the PSO-based PID controller method. PSO-based PID gain parameters in the region sought for the inverted pendulum system were determined as  $K_{pp} = 105$ ,  $K_{dp} = 34.4073$ ,  $K_{ip} = 40$ ,  $K_{pc} = 58.3944$ ,  $K_{dc} = 60$ , and  $K_{ic} = 10$ , respectively. Then, PID gain parameters were tuned with the SCA-based PID controller method. SCA-based PID gain parameters in the region sought for the inverted pendulum system were determined as  $K_{pp} = 105$ ,  $K_{dp} = 34.5676$ ,  $K_{ip} = 35.6248$ ,  $K_{pc} = 60$ ,  $K_{dc} = 60$ , and  $K_{ic} = 10$ , respectively. Finally, PID gain parameters were tuned with the GWO-based PID controller method. GWO-based PID gain parameters in the region sought for the inverted pendulum system were determined as  $K_{pp} = 105$ ,  $K_{dp} = 34.5712$ ,  $K_{ip} = 40$ ,  $K_{pc} = 58.0799$ ,  $K_{dc} = 60$ , and  $K_{ic} = 10$ , respectively.

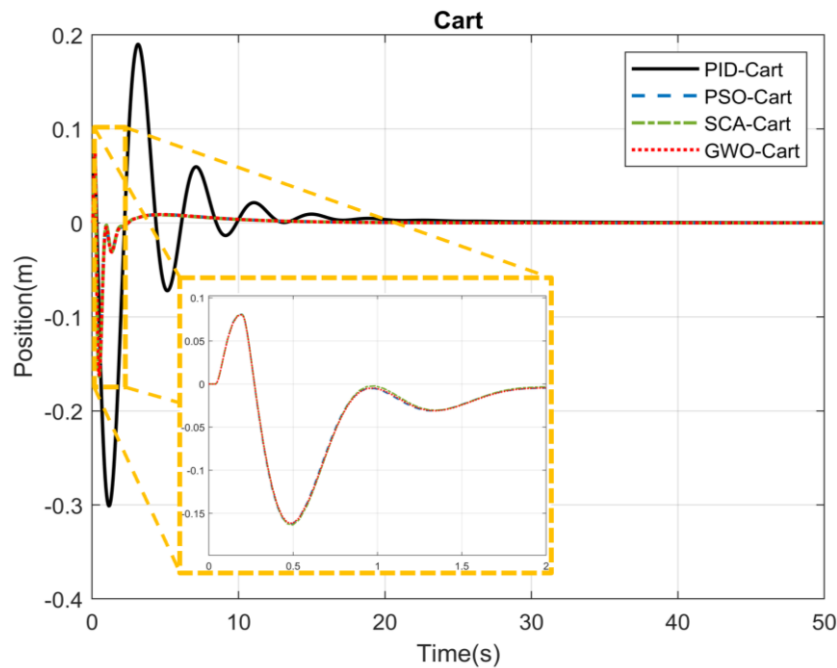


Figure 9. The controllers' responses for the cart consist of PID, PSO-PID, SCA-PID, and GWO-PID, respectively.

As a result of applying the optimized PID controllers, the pendulum's settling time reached the reference angle in 1.8138 seconds (Figure 10), while the cart's settling time reached the reference

position in 8.1721 seconds (Figure 9). As can be seen in Figure 9 and Figure 10, the peak value of the pendulum was equal to 0.2442 radians, and the peak point of the cart was determined to be -0.1673 m.

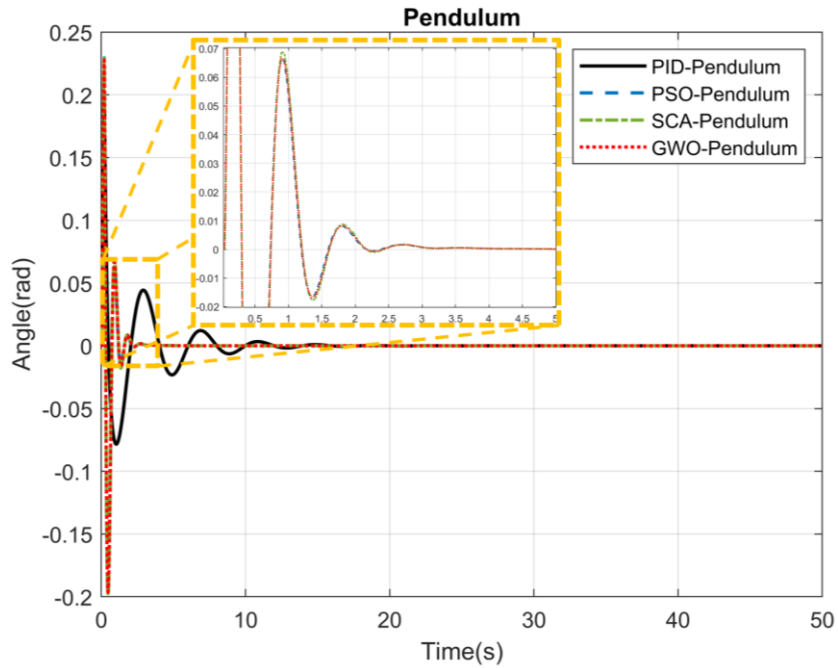


Figure 10. The controllers' responses for the pendulum consist of PID, PSO-PID, SCA-PID, and GWO-PID, respectively.

Figure 11 shows the convergence graph of the inverted pendulum system with three metaheuristic optimization algorithms. Depending on optimizing the gain parameters, the PSO-based optimized PID controller performance reached its best result in the 16th iteration. Then, the SCA-based optimized PID controller performance reached its best result in the 47th iteration. Finally, GWO achieved the best convergence result in the 9th iteration. The fastest convergence was achieved with GWO, while the slowest was achieved with SCA.

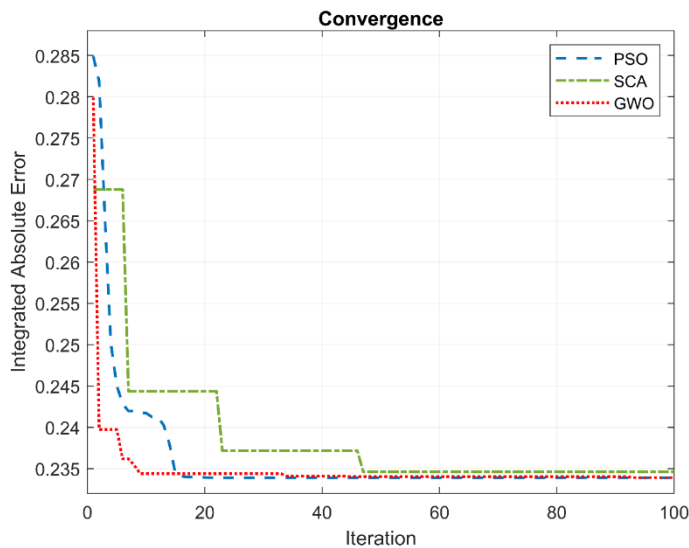


Figure 11. Convergence graph of optimized PID controllers.

The integrated absolute error (IAE) and integrated squared error (ISE) were used to compare the developed controllers' performances. Statistical error analysis results for four different controllers

are given in Table 2. While the performance of the classical PID controller increased by approximately 76% compared to IAE, an increase of approximately 79% was achieved compared to ISE. PID controller performances based on metaheuristic methods are almost close to each other. The results obtained with three different metaheuristic optimization algorithm methods are close to each other because the search regions were chosen the same. All metaheuristic methods applied in this study used 50 particles and 100 iterations.

Table 2. Comparison of performances.

| Controller Type       | IAE     | ISE     | Performance variation according to PID controller |        |
|-----------------------|---------|---------|---|--------|
|                       |         |         | IAE   | ISE    |
| <b>PID Controller</b> | 1.01700 | 0.20800 |   |        |
| <b>PSO-PID</b>        | 0.23420 | 0.04222 | %76.97  | %79.70 |
| <b>SCA-PID</b>        | 0.23550 | 0.04272 | %76.84  | %79.46 |
| <b>GWO-PID</b>        | 0.23430 | 0.04178 | %76.96  | %79.91 |

#### 4. Conclusions

In this study, it was seen that the optimization of the inverted pendulum control system was successfully carried out using the specified metaheuristic methods. The  $K_p$ ,  $K_i$ , and  $K_d$  coefficients of the PID control parameters, which are the essential elements of the control system, have been effectively optimized according to the determined criteria. The results obtained with metaheuristic algorithms performed much better than those found with the Ziegler-Nichols method. In addition, this study obtained information about the convergence speeds of PSO, SCA, and GWO methods by applying the same constraints to the PID gain parameters for the inverted pendulum system. In future studies, a more effective control process can be achieved by applying hybrid metaheuristic methods. Additionally, a better controller design can be made by considering more than one parameter of the controller by using the multi-objective function.

#### References

- [1] A. Bayram, A. S. Duru, (2022). Dynamics analysis of a head-neck rehabilitation robot using Newton-Euler equations. International Conference on Engineering Technologies (ICENTE 2022), Konya, Turkey, pp. 277-281.
- [2] J. G. Ziegler, and N. B. Nichols, (1993). Optimum settings for automatic controllers. ASME Journal of Dynamic Systems, Measurement, and Control. 115, 220–222.
- [3] R. Chotikunnan, P. Chotikunnan, A. Ma'arif, N. Thongpance, Y. Pititheeraphab, A. Srisiriwat, (2023). Ball and beam control: evaluating type-1 and interval type-2 fuzzy techniques with root locus optimization, International Journal of Robotics and Control Systems. 3,286-303.
- [4] Ö. Gündoğdu, (2005). Optimal tuning of PID controller gains using genetic algorithms. Journal of Engineering Sciences, 11(1), 131-135.
- [5] A. Jayachitra, and R. Vinodha, (2014). Genetic algorithm based PID controller tuning approach for continuous stirred tank reactor. Advances in Artificial Intelligence, 2014,1-8.
- [6] D. P. Mishra, U. Raut, A. P. Gaur, S. Swain, S. Chauhan, (2023). Particle swarm optimization and genetic algorithms for PID controller tuning. Proceedings of the 5th International Conference on Smart Systems and Inventive Technology (ICSSIT 2023), Tirunelveli, India, 2023, pp. 189-194.
- [7] H. Du, P. Liu, Q. Cui, X. Ma, H. Wang, (2022). PID controller parameter optimized by reformative artificial bee colony algorithm. Journal of Mathematics. 2022, 1-16.

- [8] Y. T. Hsiao, C. L. Chuang, and C. C. Chien, (2004). Ant colony optimization for designing of PID controllers. International Conference on Robotics and Automation (IEEE 2004), New Orleans, LA, 2004, pp. 321-326.
- [9] X. Z. Li, F. Yu, and Y. B. Wang, (2007). PSO algorithm based online self-tuning of PID controller. International Conference on Computational Intelligence and Security (CIS 2007), Harbin, China, 2007, pp. 128-132.
- [10] F. Loucif, S. Kechida, A. Sebbagh (2020). Whale optimizer algorithm to tune PID controller for the trajectory tracking control of robot manipulator. Journal of the Brazilian Society of Mechanical Sciences and Engineering. 42, 1-11.
- [11] R. Paradhan, S. K. Majhi, J. K. Pradhan, B. B. Pati, (2018). Antlion optimizer tuned PID controller based on bode ideal transfer function for automobile cruise control system. Journal of Industrial Information Integration. 9, 45-52.
- [12] B. Hekimoğlu, (2019). Sine-cosine algorithm-based optimization for automatic voltage regulator system. Transactions of the Institute of Measurement and Control. 41, 1761-1771.
- [13] J. Mercieca, and S. G. Fabri, (2012). A metaheuristic particle swarm optimization approach to non-linear model predictive control. International Journal on Advances in Intelligent Systems. 5, 357-369.
- [14] D. T. M. Phuong, P. V. Hung, N. N. Khoat, P. V. Minh, (2022). Balancing a practical inverted pendulum model employing novel metaheuristic optimization based fuzzy logic controller. International Journal of Advanced Computer Science and Applications. 13, 547-553.
- [15] N. K. Nguyen, V. N. Pham, T. C. Ho, T. M. P. Dao, (2022). Designing an effective hybrid control strategy to balance a practical inverted pendulum system. International Journal of Engineering Trends and Technology. 70, 80-87.
- [16] H. Wang, H. Zhou, D. Wang, S. Wen, (2013). Optimization of LQR controller for inverted pendulum system with artificial bee colony algorithm. International Conference on Advanced Mechatronic Systems, (IEEE 2013), Luoyang, China, pp. 158-162.
- [17] A. Mourad, Y. Zennir, C. Tolba, (2022). Intelligent and robust controller tuned with WOA: applied for inverted pendulum. Journal Européen des Systèmes Automatisés. 55, 359-366
- [18] J. Kennedy and R. Eberhart, (1995). Particle swarm optimization. International Conference on Neural Networks, Perth, WA, Australia, 1995, pp. 1942-1948.
- [19] S. Mirjalili, (2016). A sine cosine algorithm for solving optimization problems. Knowledge-Based Systems. 96, 120-133.
- [20] S. Mirjalili, S. M. Mirjalili, A. Lewis, (2014). Grey wolf optimizer. Advances in Engineering Software. 69, 46-61.